Spectrochimica Acta Part A: Molecular and Biomolecular Spectroscopy 125 (2014) 375–383

Contents lists available at ScienceDirect

Spectrochimica Acta Part A: Molecular and Biomolecular Spectroscopy

journal homepage: www.elsevier.com/locate/saa

Ruthenium(II) bipyridine complexes bearing quinoline–azoimine (NN′N″) tridentate ligands: Synthesis, spectral characterization, electrochemical properties and single-crystal X-ray structure analysis

Mousa Al-Noaimi [a,*], Obadah S. Abdel-Rahman [b], Ismail I. Fasfous [a], Mohammad El-khateeb [c], Firas F. Awwadi [d], Ismail Warad [e]

[a] Department of Chemistry, Hashemite University, P.O. Box 150459, Zarqa 13115, Jordan
[b] Fachbereich Chemie der Universität Konstanz, Universitätstraße 10, D-78457 Konstanz, Germany
[c] Chemistry Department, Faculty of Science and Arts, Jordan University of Science and Technology, Irbid 22110, Jordan
[d] Department of Chemistry, The University of Jordan, Amman 11942, Jordan
[e] Department of Chemistry, AN-Najah National University, Nablus, Occupied Palestinian Territory

HIGHLIGHTS

- New azoimine–quinoline (L—Y) tridentate ligands are synthesized.
- Mixed-ligand [Ru^{II}(L–Y)(bpy)Cl](PF_6) complexes are synthesized and characterized.
- The absorption spectrum was modeled by TD-DFT.

GRAPHICAL ABSTRACT

Four octahedral ruthenium(II) azoimine–quinoline complexes having the general molecular formula [Ru^{II}(L—Y)(bpy)Cl](PF_6) {L—Y = $YC_6H_4N{=}NC(COCH_3){=}NC_9H_6N$, Y = H (**1**), CH_3 (**2**), Br (**3**), NO_2 (**4**) and bpy = 2,2′-bipyrdine} were synthesized. The azoimine–quinoline based ligands behave as NN′N″ tridentate donors and coordinated to ruthenium via azo-N′, imine-N′ and quinolone-N″ nitrogen atoms. The composition of the complexes has been established by elemental analysis, spectral methods (FT-IR, electronic, ^{1}H NMR, UV/Vis and electrochemical (cyclic voltammetry) techniques. The crystal structure of complex **1** is reported. The Ru(II) oxidation state is greatly stabilized by the novel tridentate ligands, showing Ru(III/II) couples ranging from 0.93–1.27 V *vs.* Cp_2Fe/Cp_2Fe^+. The absorption spectrum of **1** in dichloromethane was modeled by time-dependent density functional theory (TD-DFT).

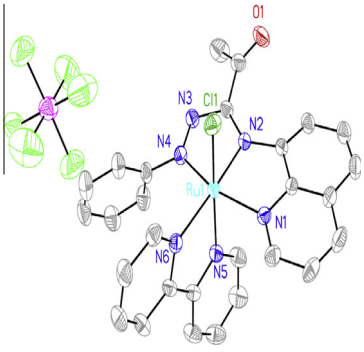

ARTICLE INFO

Article history:
Received 22 October 2013
Received in revised form 8 January 2014
Accepted 14 January 2014
Available online 5 February 2014

ABSTRACT

Four octahedral ruthenium(II) azoimine–quinoline complexes having the general molecular formula [Ru^{II}(L—Y)(bpy)Cl](PF_6) {L—Y = $YC_6H_4N{=}NC(COCH_3){=}NC_9H_6N$, Y = H (**1**), CH_3 (**2**), Br (**3**), NO_2 (**4**) and bpy = 2,2′-bipyrdine} were synthesized. The azoimine–quinoline based ligands behave as NN′N″ tridentate donors and coordinated to ruthenium via azo-N′, imine-N′ and quinolone-N″ nitrogen atoms. The composition of the complexes has been established by elemental analysis, spectral methods (FT-IR, electronic, ^{1}H NMR, UV/Vis and electrochemical (cyclic voltammetry) techniques. The crystal structure of

* Corresponding author. Tel.: +962 (5) 3903333; fax: +962 (5) 3826613.
E-mail address: manoaimi@hu.edu.jo (M. Al-Noaimi).

http://dx.doi.org/10.1016/j.saa.2014.01.075
1386-1425/

complex **1** is reported. The Ru(II) oxidation state is greatly stabilized by the novel tridentate ligands, showing Ru(III/II) couples ranging from 0.93–1.27 V *vs.* Cp_2Fe/Cp_2Fe^+. The absorption spectrum of **1** in dichloromethane was modeled by time-dependent density functional theory (TD-DFT).

Keywords:
Ruthenium
Azoimine–quinoline ligands
Spectroelectrochemistry
Electrochemistry
DFT calculation

Introduction

The study of spectroscopic, electrochemical and luminescence properties of Ru(II) polypyridine metal complexes is an ongoing and active area of research [1], primarily because of the fascinating redox, photophysical and photochemical properties exhibited by such complexes. As the properties are dependent mostly on the coordination environment around the metal center, ruthenium monoterpyridine complexes of the type [Ru(trpy)(L)] incorporating different kinds of ancillary ligands (L) have been synthesized [2]. In most cases, the ligands L are heterocyclic bidentate imines involving pyridine, pyrazine, pyrimidine or quinoline rings [3] and tridentate NN′N″ type ligands [4]. Recently, strong π-acidic azo-imine function {L = $NC_5H_4N{=}NC_6H_4(R)$} was introduced into the [Ru(trpy)] core to modulate their properties [5]. The chemically generated oxo-complexes, $[Ru^{IV}(trpy)(L)(O)]^{2+}$ are found to be active catalysts for the facile oxidation of water to dioxygen [6].

8-Aminoquinoline is a pyridine derivative in which aniline is fused with pyridine so that a NN′ chelating ligand may be generated. It is a common ligand for transition metal complexes [7] and can co-ordinates to a metal as bi-dentate ligand [7,8]. The ratio of metal to 8-aminoquinoline in a co-ordination complex depends on several factors such as the size of the metal ion and the affinity of 8-aminoquinoline to the metal ion.

Recently, we have adopted a simple technique to synthesis bidentate azoimine ligands (K) (where K is Ph–N=N–C(R)=N–Ph) by reacting hydrazonyl chloride with an appropriate aniline derivative [9–15]. The electronic properties of these ligands can be modified significantly by changing the substituents R and the substituent on the phenyl rings. These ligands are capable of stabilizing metals in their low oxidation state like Ru(II) in which the degree of stabilization depends on both the substituent on Ph and R groups [9–15]. Recently, we reported the synthesis of Ru(II) complexes of novel tetradentate (NSN′N″) pyridylthioazoimine ligands, containing a hard donor azo-N, imine-N′, pyridine-N″ and soft thioether-S donors [9]. Herein, the novel family of four tridentate azoimine–quinoline of the type NN′N″ (H_2L—Y) and mononuclear mixed–ligand ruthenium complexes of the type $[Ru^{II}(L{-}Y)(bpy)Cl](PF_6)$ {L—Y = $YC_6H_4N{=}NC(COCH_3){=}NC_9H_6N$, Y = H (**1**), CH_3 (**2**), Br (**3**), NO_2 (**4**) and bpy is 2,2′-bipyridine} have been prepared. These new ligands offer the combination of moderate π-acceptor [18] pyridine nitrogen (N″) and a good π-acceptor [9–15] azoimine moiety (N and N′). Thus this combination should in principle afford complexes with tunable spectroscopic and redox properties. The effect of the substituent Y of the ligands L—Y on the electronic properties of the resulting mononuclear ruthenium complexes was studied by spectroscopic and electrochemical methods.

Experimental

Materials

The reagents: ruthenium trichloride, lithium chloride, ammonium hexafluorophosphate, tetrabutylammonium hexafluorophosphate (TBAHF), and solvents (reagent grade) were purchased from Aldrich. All hydrazonyl chlorides were prepared according to published procedure [8].

Preparation of (H_2L—Y); General procedure

To a solution (20 mmol) of appropriate hydrazonyl chloride in 5.0 mL absolute ethanol, (2.86 g, 20 mmol) of 8-aminoqunoline and triethylamine (2.4 g, 24 mmol) were added. The reaction mixture was refluxed for 2 h, condensing the solution followed by cooling produced a yellow solid which was recrystallized from ethanol.

(1Z)-2-oxo-N′-phenyl-N-quinolin-8-ylpropanehydrazonamide (H_2L—H)

Yield. (3.2 g, 52%). Anal. Calc. for $C_{18}H_{16}N_4O$: C, 71.04; H, 5.30; N, 18.41. Found: C, 71.21; H, 5.20; N, 18.31%. UV–Vis in dichloromethane: λ_{max}(nm) ($\varepsilon_{max}/M^{-1}\,cm^{-1}$): 241 ($69.77 \times 10^4$), 299 ($32.27 \times 10^4$), 352 ($45.65 \times 10^4$). IR: ν(C=N) 1577, ν(C=O) 1668 cm^{-1}. ^1H NMR ($CDCl_3$, δ ppm): 8.90 (d, 1H, H10), 8.49 (s, 1H, NH), 8.15 (d, 1H, H5), 7.70 (s, 1H, NH), 7.50 (t, 1H, H9), 7.40 (d, 2H, H2, H3), 7.35 (m, 3H, Y = H, H7, H6), 7.05 (d, 2H, H1, H4), 6.35 (d, 1H, H8), 2.62 (s, 3H, $COCH_3$). m.p is 161–162 °C.

(1Z)-N′-(4-methylphenyl)-2-oxo-N-quinolin-8-ylpropanehydrazonamide (H_2L—CH_3)

Yield. (3.9 g, 61%). Anal. Calc. for $C_{19}H_{18}N_4O$: C, 71.68; H, 5.70; N, 17.60. Found: C, 71.50; H, 5.62; N, 17.75%. UV–Vis in dichloromethane: λ_{max}(nm) ($\varepsilon_{max}/M^{-1}\,cm^{-1}$): 243 ($68.5 \times 10^4$), 303 ($32.4 \times 10^4$), 359 ($44.5 \times 10^4$). IR: ν(C=N) 1599, ν(C=O) 1674 cm^{-1}. 1H NMR ($CDCl_3$, δ ppm): 8.92 (d, 1H, H10), 8.48 (s, 1H, NH), 8.2 (d, 1H, H5), 7.72 (s, 1H, NH), 7.50 (m, 1H, H9), 7.45 (d, 2H, H2, H3), 7.10 (m, 2H, H6, H7, H10), 7.05 (d, 2H, H1, H4), 6.35 (d, 1H, H8), 2.62 (s, 3H, $COCH_3$), 1.1 (s, 3H, CH_3). m.p. is 120–121 °C.

(1Z)-N′-(4-bromophenyl)-2-oxo-N-quinolin-8-ylpropanehydrazonamide (H_2L—Br)

Yield. (4.97 g, 65%). Anal. Calc. for $C_{18}H_{15}BrN_4O$: C, 56.41; H, 3.95; N, 14.62. Found: C, 56.53; H, 3.78; N, 14.54%. UV–Vis in dichloromethane: λ_{max}(nm) ($\varepsilon_{max}/M^{-1}\,cm^{-1}$): 245 ($69.02 \times 10^4$), 297 ($31.50 \times 10^4$), 380 ($44.5 \times 10^4$). IR: ν(C=N) 1578, ν(C=O) 1673 cm^{-1}. 1H NMR (CDCl3, δ ppm): 8.92 (d, 1H, H10), 8.50 (s, 1H, NH), 8.18 (d, 1H, H5), 7.65 (s, 1H, NH), 7.50 (m, 1H, H9), 7.45 (d, 2H, H2, H3), 7.35 (m, 2H, H6, H7), 7.05 (d, 2H, H1, H4), 6.35 (d, 1H, H8), 2.62 (s, 3H, $COCH_3$). m.p. is 164–165 °C.

(1Z)-N′-(4-nitrophenyl)-2-oxo-N-quinolin-8-ylpropanehydrazonamide (H_2L—NO_2)

Yield. (4.88 g, 70%). Anal. Calc. for $C_{18}H_{15}N_5O_3$: C, 61.89; H, 4.33; N, 20.05. Found: C, 61.73; H, 4.48; N, 20.24%. UV–Vis in dichloromethane: λ_{max}(nm) ($\varepsilon_{max}/M^{-1}\,cm^{-1}$): 235 ($68.8 \times 10^4$) 33.2 ($5.38 \times 10^4$), 405 ($69.1 \times 10^4$). IR: ν(C=N) 1578, ν(C=O) 1675 cm^{-1}.^1H NMR ($CDCl_3$, δ ppm): 8.89 (d, 1H, H10), 8.40 (s, 1H,

NH), 8.10 (d, 1H, H5), 7.69 (s, 1H, NH), 7.45 (m, 1H, H9), 7.35 (m, 2H, H6, H7), 7.05 (d, 2H, H2, H3), 7.00 (d, 2H, H1, H4), 6.29 (d, 1H, H8), 2.60 (s, 3H, $COCH_3$). m.p. is 209–210 °C.

Preparation of [Ru(bpy)(L—Y)Cl]PF_6; General procedure

To a solution of ruthenium trichloride trihydrate (261 mg, 1.0 mmol) in 100 mL of absolute ethanol, (1.0 mmol) of (H_2L—Y) were added. After refluxing for 1 h, 1.0 mmol of 2,2′-bipyridine was added to the solution. The reaction was heated for an additional 2 h then an excess amount of LiCl (500 mg, 11.8 mmol) was added. After allowing the reaction mixture to reflux for an additional 1 h, the solvent was then removed by a rotary evaporator. The volume was reduced to approximately 30 mL and then an excess saturated aqueous solution of NH_4PF_6 was added to it to precipitate the crude product. The crude product was filtered out and washed with water to remove the excess NH_4PF_6 and unreacted ruthenium trichloride and lithium chloride. The crude product was then dried and dissolved in 20 mL (2:1) dichloromethane/acetonitrile and purified by chromatography on a 50 cm long, 3 cm diameter column containing 250 g grade (III) alumina (Brockman I, weakly acidic 150 mesh). The first yellow band, thought to be the ligand L—Y, was eluted with dichloromethane. The second dark red band, which was the complex, was eluted with (1:1) dichloromethane:acetonitrile.

*[Ru(bpy)(L—H)Cl_2](PF_6) (**1**)*

Yield. (0.33 g, 44%). Anal. Calc. for $C_{28}H_{22}N_6OClF_6PRu$: C, 45.45; H, 3.00; N, 11.36%. Found: C, 45.30; H, 2.92; N, 11.45%. UV–Vis in dichloromethane: λ_{max}(nm) (ε_{max}/M^{-1} cm^{-1}): 242 (6.0×10^4), 284 (4.7×10^4), 365 (2.6×10^4), 434 (2.3×10^4), 512 (1.6×10^4). IR: ν(N═N) 1473, ν(C═N) 1605, ν(C═O) 1707 cm^{-1}. ^{1}H NMR (CD_2Cl_2, δ ppm): 9.72 (d, 1H, H11), 9.01 (d, 1H, H10), 8.47 (d, 1H, H18), 8.29 (m, 3H, H5, H6, H7), 8.04 (d, 1H, H14), 7.87 (m, 1H, H16), 7.82 (t, 1H, H9), 7.68 (t, 1H, H12),7.53 (m, 2H, H17), 7.31 (m, 2H, H13, H15), 7.22 (t, 2H, H6, H8), 7.15 (d, 2H, H2, H3), 7.05 (m, 3H, H1, H4, Y═H). 2.62 (s, 3H, $COCH_3$), ^{19}F-NMR (CD_2Cl_2, δ ppm): −72.10 (s), −73.99 (s).

*[Ru(bpy)(L-CH_3)Cl_2](PF_6) (**2**)*

Yield. (0.33 g, 42%). Anal. Calc. for $C_{29}H_{24}ClF_6N_6OPRu$: C, 46.19; H, 3.21; N, 11.15%. Found: C, 46.24; H, 3.24; N, 11.25%. UV–Vis in dichloromethane: λ_{max}(nm) (ε_{max}/M^{-1} cm^{-1}): 246 (4.3×10^4), 282 (4.0×10^4), 368 (2.4×10^4), 443 (2.3×10^4), 515 (broad) (2.0×10^4). IR: ν(N═N) 1465, ν(C═N) 1605, ν(C═O) 1695 cm^{-1}. ^{1}H NMR (CD_2Cl_2, δ ppm): 8.95 (d, 1H, H11), 8.49 (d, 1H, H18), 8.29 (m, 2H, H12, H13), 8.24 (d, 1H, H8), 8.01 (d, 1H, H14), 7.85 (m, 3H, H6, H7, H9), 7.67 (m, 1H, H6), 7.28 (d, 2H, H2, H3), 7.20 (m, 3H, H10, H5, H16), 7.14 (d, 2H, H17, H15), 6.84 (d, 2H, H1, H4), 2.68 (s, 3H, $COCH_3$), 1.1 (s, 3H, CH_3). ^{19}F NMR (CD_2Cl_2, δ ppm): −2.16 (s), −74.05 (s).

*[Ru(bpy)(L—Br)Cl_2](PF_6) (**3**)*

Yield. (0.37 g, 45%). Anal. Calc. for $C_{28}H_{21}BrN_6OClF_6PRu$: C, 41.07; H, 2.58; N, 10.26%. Found: C, 41.27; H, 2.54; N, 10.35%. UV–Vis in dichloromethane: λ_{max}(nm) (ε_{max}/M^{-1} cm^{-1}): 242 (6.0×10^4), 285 (4.7×10^4), 364 (2.6×10^4), 434 (2.4×10^4), 514 (broad) (1.6×10^4). IR: ν(N═N) 1473, ν(C═N) 1605, ν(C═O) 1708 cm^{-1}. ^{1}H NMR (CD_2Cl_2, δ ppm): 9.75 (d, 1H, H11), 9.00 (d, 1H, H18), 8.48 (d, 1H, H10), 8.31 (t, 1H, H17), 8.25 (t, 1H, H16), 8.05 (d, 1H, H5), 7.88 (m, 2H, H7, H8), 7.69 (t, 1H, H6), 7.26 (d, 2H, H2, H3), 7.24 (d, 2H, H1, H4), 7.24 (m, 5H, H9, H12, H13, H14, H15), 2.65 (s, 3H, $COCH_3$), ^{19}F NMR (CD_2Cl_2, δ ppm): −72.08 (s), −73.97 (s).

*[Ru(bpy)(L—NO_2)Cl_2] (**4**)*

Yield. (0.31 g, 40%). Anal. Calc. for $C_{28}H_{21}N_7O_3ClF_6PRu$: C, 42.84; H, 2.70; N, 12.49%. Found: C, 42.74; H, 2.78; N, 12.55%. UV–Vis in dichloromethane: λ_{max}(nm) (ε_{max}/M^{-1} cm^{-1}): 242 (2.0×10^4), 289 (2.4×10^4), 367 (8.4×10^3), 449 (7.8×10^3), 510 (1.6×10^3). IR: ν(N═N) 1467, ν(C═N) 1604, ν(C═O) 1704 cm^{-1}. ^{1}H NMR (CD_2Cl_2, δ ppm): 9.68 (d, 1H, H11), 9.07 (d, 1H, H18), 8.49 (d, 1H, H10), 8.34 (m, 3H, H17, H16, H5), 7.98 (t, 1H, H9), 7.9 (m, 3H, H12, H15, H14), 7.70 (m, 1H, H6), 7.54 (m, 2H, H6, H7),7.37(d, 2H, H2, H3), 7.25 (d, 2H, H1, H4), 7.19 (m, 2H, H8, H13), 2.62 (s, 3H, $COCH_3$). ^{19}F NMR (CD_2Cl_2, δ ppm): −71.77 (s), −73.66(s).

Instrumentation

^{1}H NMR (400 MHz) and ^{31}P NMR (162 MHz) spectra were measured on a Bruker Avance III 400 spectrometer as CD_2Cl_2 solutions at room temperature. All chemical shifts are reported in ppm downfield of TMS (1H) or 85% phosphoric acid (^{31}P) and referenced using the chemical shifts of residual solvent resonances. IR spectra were measured by FT-IR JASCO model 420. Elemental analyses were carried out on a Eurovector E.A.3000 instrument using copper sample-tubes. UV–Vis/NIR spectra were recorded on a TIDAS fiberorptic diode array spectrometer (combined MCS UV/NIR and PGS NIR instrumentation) from j&m in HELLMA quartz cuvettes with 0.1 cm optical path lengths. Electrochemical measurements were performed in dichloromethane (Aldrich, HPLC grade) using BAS CV-27. All electrochemical experiments were done in a home-built cylindrical vacuum-tight one-compartment cell. A spiral-shaped Pt wire and an Ag wire as the counter and thin pseudo-reference electrodes are sealed into glass capillaries via standard joints and fixed by Quickfit screws. A platinum electrode is introduced as the working electrode through the top central port *via* a Teflon screw cap with a suitable fitting. It is polished with first 1 μm and then 0.25 μm diamond pastes before measurements. The cell was attached to a conventional Schlenk line *via* a side arm equipped with a Teflon screw valve and allows experiments to be performed under argon atmosphere with approximately 5 mL of analyte solution. Tetrabutylammonium hexafurophosphate (TBAHF) (0.1 M) was twice recrystallized and vacuum dried at 120 °C, and used as the supporting electrolyte. The temperature was controlled (at 25.0 ± 0.1 °C) by a Haake D8-G refrigerator. Referencing was done with an addition of one crystal of decamethylferrocene (Cp^*_2Fe) as an internal standard to the analyte solution after all data of interest had been acquired. Representative sets of scans were repeated with the added standard. A final referencing was done against the ferrocene/ferrocenium ($Cp_2Fe^{0/+}$) couple with $E_{1/2}Cp^*_2Fe^{0/+} = -542$ mV vs. $Cp_2Fe^{0/+}$ [16,17]. Spectroelectrochemistry of a representative complex **1** was performed by using an optically transparent thin layer electrochemistry (OTTLE) cell [18]. OTTLE cell was home-built and comprises a Pt working and counter electrode and a thin silver wire as a pseudo-reference electrode sandwiched between two CaF_2 windows of a conventional liquid IR cell. The working electrode is positioned in the center of the spectrometer beam. The potential was controlled by the same BAS CV-27 that was used for cyclic voltammetry. At any given potential, the system was allowed to come to equilibrium ($i \sim 0$ A) before the spectrum was taken.

Computational methods

Full geometry optimization of **1** was carried out using density functional theory (DFT) at the B3LYP level [19]. All calculations were carried out using the GAUSSIAN 03 program package with the aid of the GaussView visualization program [20]. For C, H, Cl, N and P the 6–31G(d) basis set were assigned, while for Ru, the

LanL2DZ basis set with effective core potential were employed [21]. Vertical electronic excitations based on B3LYP optimized geometries were computed using the time-dependent density functional theory (TD-DFT) formalism in dichloromethane using conductor-like polarizable continuum model (CPCM) [22–25]. Gauss Sum was used to calculate the fractional contributions of various groups to each molecular orbital [26].

Crystallography

A suitable irregular brown flat fragment of approximate dimensions 0.25 × 0.15 × 0.10 mm^3 of complex **1** was mounted on a glass fiber and the data collected at room temperature employing enhanced Mo radiation, λ = 0.71073 Å, using Xcalibur/Oxford Diffractometer equipped with Eos CCD detector. CrysAlis Pro software was used for data collection, absorption correction and data reduction to give SHELX-format-*hkl* files, [27]. 'Multi-scan' absorption corrections were applied with Min and Max transmission factors of 0.692 and 1.000 respectively [27]. Cell parameters were retrieved using 2707 reflections. The structure was solved using SHELXTL program package [28]. All nonhydrogen atoms were refined anisotropically except hydrogen atoms which were placed in calculated positions and refined using a riding model; they assigned isotropic thermal parameters of 1.2 times that of the riding atoms. Details of data collection and refinement are given in Table 1. An ORTEP drawing of the asymmetric unit (30% probability) is given in Fig. 1.

Results and discussion

Synthesis

The primary objective of the present study has been to synthesize a group of mixed-ligand complexes of ruthenium containing both 2,2′-bipyridine and azoimine–quinoline based NN′N″ ligands (L—Y) {L—Y = $YC_6H_4N{=}NC(COCH_3){=}NC_9H_6N$). For this purpose, four H_2L—Y with different substituents (Y = H, CH_3, Br and NO_2) at the para position of the phenyl rings have been used in order to study their influence, if any, on the redox properties of the resulting ruthenium complexes. These azoimine–quinoline based ligands are abbreviated in general as H_2L—Y, where H_2 stands for the two dissociable protons and Y for the substituents. The Four azoimine–quinoline ligands (H_2L—Y) were prepared by reacting 8-aminoquinoline with the appropriate hydrazonyl chloride in refluxing ethanol (Scheme 1). Pure products were obtained as yellow crystals by recrystallization from ethanol and they were characterized by ^{1}H NMR spectroscopy and elemental analyses. These organic compounds act as tridentate NN′N″ ligands, which are interesting chelators due to the presence of hard donor azo-N and imine-N′ and borderline base pyridine-N″.

Table 1
Crystallographic data and structure refinement parameters for **1**.

	Complex **1**
Empirical formula	$C_{28}H_{22}ClF_6N_6OPRu$
Formula weight	740.01
Temperature	293(2) K
Wavelength	0.71073 Å
Crystal system	Monoclinic
Space group	*P* 1 21/*n* 1
Unit cell dimensions	*a* = 8.2663(3) Å
	b = 17.0078(6) Å
	c = 21.1752(6) Å
Volume	2933.92(17) Å^3
Z	4
Density (calculated)	1.673 Mg/m^3
Absorption coefficient	0.750 mm^{-1}
F(0 0 0)	1484
Crystal size	0.25 × 0.15 × 0.1 mm^3
Theta range for data collection	3.09–25.00°
Index ranges	$-9 \leftarrow h \leftarrow 9$, $-20 \leftarrow k \leftarrow 13$, $-23 \leftarrow l \leftarrow 25$
Reflections collected	12,338
Independent reflections	5162 [*R*(int) = 0.0344]
Completeness to theta = 25.00°	99.8%
Absorption correction	Semi-empirical from equivalents
Max. and min. transmission	1.00000 and 0.69229
Refinement method	Full-matrix least-squares on F^2
Data/restraints/parameters	5162/0/397
Goodness-of-fit on *F*2	1.036
Final *R* indices [*I* > 2sigma(*I*)]	R_1 = 0.0446, wR_2 = 0.0971
R indices (all data)	R_1 = 0.0661, wR_2 = 0.1098
Largest diff. peak and hole	0.668 and −0.409 e Å^{-3}

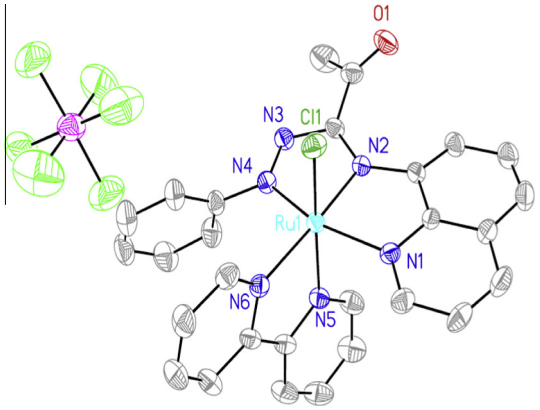

Fig. 1. Thermal ellipsoid drawing (30%) of complex **1**.

The ruthenium (II) complexes of these ligands were obtained by the reaction of H_2L—Y with equimolar amounts of $RuCl_3$ in refluxing ethanol. It may be noted here that during the synthetic reaction ruthenium has undergone a one-electron reduction. Ethanol presumably acts both as a solvent and as a reducing agent for Ru(III). The H_2L—Y are oxidized to L—Y by Ru(III) (Scheme 1). For the ligands, the N—H protons appear as two singlets around 8.5 and 7.2–7.6 ppm, and these signals are absent in all of the complexes, indicating the full oxidation of NH to azo and imine groups and the coordination of these nitrogens to the metal center. The aromatic region in the ^{1}H NMR spectra of complexes **1**–**4** consists of several coupled multiplets due to the aromatic protons of the phenyl rings of the azoimine-qinoline and 2,2′-bipyridine ligands.

All the complexes are air stable as solids or in solution and are soluble in common organic solvents such as acetone, dichloromethane, acetonitrile, dimethyl formamide, dimethyl sulfoxide, etc., and producing intense colored solutions. Preliminary (microanalytical, spectroscopic, magnetic, etc.) characterizations on these complexes (*vide infra*) are found to be in well accordance with their compositions. In order to find out coordination mode of the ligands L—Y in these complexes, structure of a representative member of this family, complex **1** has been determined by X-ray crystallography. The molar conductivities (Λ_M) of these compounds are in the range 116–140 Ω^{-1} cm^2 mol^{-1} in CH_3CN, consistent with their 1:1 electrolyte natures. The diamagnetic behavior of all compounds indicates that ruthenium is in + 2 oxidation state with a low spin d^6 system.

The FT-IR spectra of the of free H_2L—Y showed bands in the regions of 3100–3250 cm^{-1}, 1577–1596 cm^{-1} and 1668–1673 which are assigned to NH group of quinoline and NH group of hydrazonylchloride, C=N group of quinolone and C=O of the acetyl groups, respectively. The IR spectra of complexes **1**–**4** exhibit a sharp intense bands at 1695–1705 cm^{-1}, 1580–1610 and 1470–1490 cm^{-1} which correspond to acetyl group, C=N and N=N stretching bands, respectively. A broad band in the IR spectra at 825 cm^{-1} for complexes **1**–**4** confirms the presence of PF_6 ion.

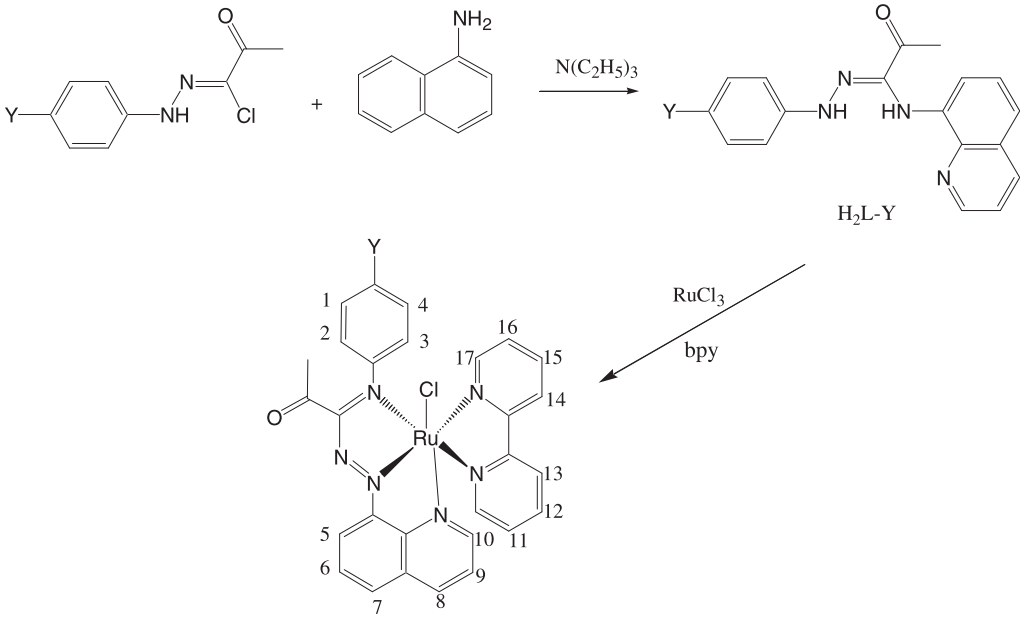

Y=H, **1**; Y=CH_3, **2**; Y=Br, **3**; Y=NO_2, **4**

Scheme 1. Synthesis of [Ru(L—Y)(bpy)Cl](PF_6) complexes.

Hence, from the infrared spectroscopic data, it was inferred that azomethine, and quinoline nitrogen atoms are involved in the coordination of the tridentate ligand to ruthenium ion in all the complexes.

Crystal structure

Single crystal structure of **1** is shown in Fig. 1 and selected bond parameters are listed in Table 1. Complex **1** crystallizes in the monoclinic space group P $2_1/n$. The structure shows that the H_2L—H is coordinated to ruthenium, *via* dissociation of two acidic protons, as a tridentate N,N′,N″-donor. L—H ligand is co-ordinated in the expected meridional fashion with the ligand bpy in *cis* orientation [29]. The RuN_5Cl co-ordination spheres in **1** is distorted octahedral as can be seen from the angles subtended at the metal ions (Table 2). In the crystal lattice of the [Ru^{II}(bpy)(L—H)Cl](PF_6) complex, there is one molecule of PF_6 per one complex molecules.

The average bond length for Ru—N (bpy) is 2.078 Å. The five membered rings described by the coordination of an azoimine (N4—Ru—N2), iminepyridine N(2)—Ru(1)—N(1) and bpy N(5)—Ru(1)—N(6) are (78.53(14)), 81.88(13) and 77.61(14) respectively. The geometrical constraints imposed on the meridional L—H ligand are reflected in the *trans* angles, N(1)—Ru—N(4), 159.69(14)° for **1**. The azomethine ligand is known to interact strongly with the Ru(II) center via the dπ–π^* interactions [9–15]. This has been reflected in the average Ru—N4(Azo) (1.945(3) Å) and the Ru—N2(methine) (1.960(3) Å). The shortening in the bond length for Ru–azoimine fragment compared to Ru—N(pyridine) (N(1)) bond distances (2.071(3) Å) indicates that the M—L π interaction is localized in the M–Azo fragment [9–16,30]. The chloride ligand is *trans* to the bpy and the Ru^{II}—Cl distance, 2.359(12) Å, in complex **1** is close to those found in other Ru^{II}–trpy complexes [31].

The N=N bond length is 1.313(4) Å, which is slightly longer than the bond length for the free azo (N=N) (1.266(3) Å [32], which may be due to charge delocalization from Ru(II) to the π-acidic azo group. However, it is interesting to note that the bond lengths Ru—N(Azo) and Ru–(methine) for complex **1** are slightly shorter than the corresponding lengths for similar reported ruthenium azoimine bidentate complexes, *trans*-[Ru(Azo)(t-bpy)Cl_2] (Ru—N(azo) = 1.958 (4) Å Ru—N(methine) = 1.988(4) Å and N=N is 1.252(11) Å [33]) and *trans*-[Ru(Az)(bpy)Cl2] (Ru—N(azo) = 1.965(3) Å, Ru—N(imine) = 2.002(3) Å [34]). The shortening for Ru—N(Azo) and the lengthen for N=N suggest that the ligand

Table 2
Bond lengths (Å) and angles (°) for complex **1**.

	Experimental	Calculated
Bond length (Å)		
Ru(1)—N(4)	1.945(3)	1.902
Ru(1)—N(2)	1.960(3)	1.923
Ru(1)—N(5)	2.057(4)	2.035
Ru(1)—N(1)	2.071(3)	2.025
Ru(1)—N(6)	2.100(3)	2.050
Ru(1)—Cl(1)	2.359(12)	2.285
N(4)—N(3)	1.313(4)	1.276
Bond angle (°)		
N(4)—Ru(1)—N(2)	78.53(14)	79.45
N(4)—Ru(1)—N(5)	92.09(14)	93.45
N(2)—Ru(1)—N(5)	100.73(14)	102.62
N(4)—Ru(1)—N(1)	159.69(14)	160.05
N(2)—Ru(1)—N(1)	81.88(13)	83.79
N(5)—Ru(1)—N(1)	86.29(14)	88.06
N(4)—Ru(1)—N(6)	96.94(13)	93.13
N(2)—Ru(1)—N(6)	175.17(13)	177.13
N(5)—Ru(1)—N(6)	77.61(14)	78.84
N(1)—Ru(1)—N(6)	102.47(13)	100.49

Table 3
Electrochemical data for the complexes in CH_2Cl_2/TBAHF (0.1 mM) at 25 °C; potential (mv) are given relative to the Cp_2Fe/Cp_2Fe^+.

Complex	Ru(III/II)[a]	Azo(0/−2)	bpy(0/−1)[b]	MLCT (nm)
1	0.98	−1.30	−1.71	512
2	0.93	−1.29	−1.73	515
3	1.12	−1.30	−1.73	514
4	1.27	−1.31	−1.73	510

[a] Ru(III/II) = $(E^{\circ}_{pa} + E^{\circ}_{pc})/2$.
[b] The cathodic peak maximum.

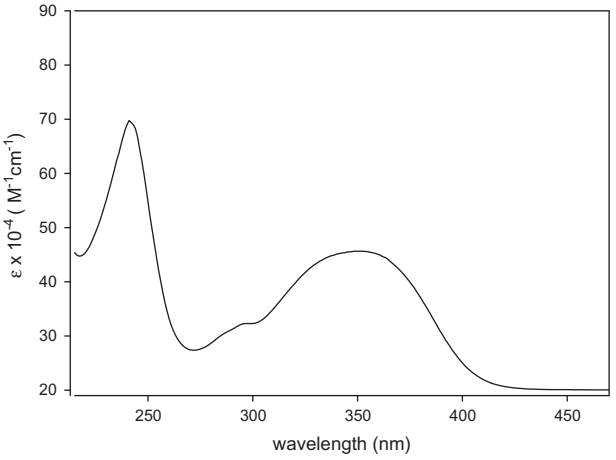

Fig. 2. UV–Vis spectrum for H_2L—H in dichloromethane.

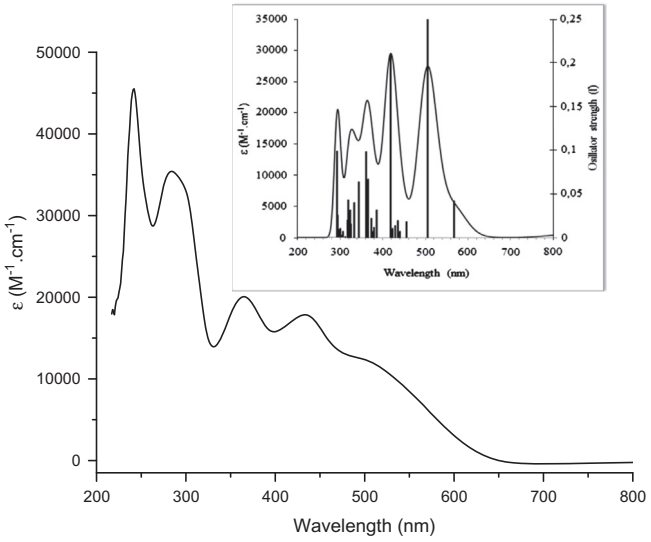

Fig. 3. UV–Vis spectrum for **1** in dichloromethane. Inset shows simulated absorption spectrum. (black line) based on TD-DFT calculations, compared to excitation energies and oscillator strengths.

L–H is better π-acceptor ligand comparing to the previously prepared azomine bidentate ligand [33,34].

Electronic structure

The electronic absorption spectra of the azoimine–quinoline ligands (H_2L—Y) and their complexes (**1**–**4**) were recorded at room temperature using dichloromethane as the solvent, and the results are shown in Table 3. The spectra of H_2L—H (Fig. 2) and complex **1** (Fig. 3) as representative examples are very similar in shape and intensity and show three well-resolved azoimine–quinoline based Ligands charge (LC) transitions in the UV region between 320 nm and 350 nm [35,36]. In addition to the bands in the UV region, The complexes display multiple transitions in the visible region (400–600 nm). Multiple charge transfer transitions may arise from lower symmetry splitting of the metal level, the presence of different acceptor orbitals and from mixing of singlet and triplet configurations in the excited state through spin–orbit coupling [37].

The assignment of the transitions in the UV–Vis region is supported by the TD-DFT calculations on a representative complex **1**. The optimized structure of complex **1** is developed using GAUSSIAN 03 analyses package [20]. The structural agreement has been observed from the comparison of bond distances and angles between calculated and X-ray determined structure (Table 2). Computation of 40 excited states of complex **1** allowed the interpretation of the experimental spectra for the complexes in the 300–800 nm range (Fig. 3). The calculated energy of excitation states and transition oscillator strength (*f*) are shown in Table 5. The absorption spectrum of **1** was simulated using Gaussian Sum software [26] based on the obtained TD-DFT results. Each excited state was interpolated by a Gaussian convolution with the full width at half-maximum (fwhm) of 3000 cm^{-1}. Both the experimental UV–Vis spectrum of complex **1** reported in dichloromethane and its simulated absorption spectrum shown in Fig. 3 were in acceptable agreement. Relative percentages of atomic contributions to the lowest unoccupied and highest occupied molecular orbitals have been placed in Table 4. Moreover, the isodensity plots for the HOMOs and LUMOs orbitals are shown in Fig. 4. For complex **1**, LUMO+1 to LUMO+3 are constructed from the π^* orbitals of azoimine ligands while LUMO+4 to LUMO+5 are constructed mainly from bpy. One particular point of interest, emphasized by Gorelsky et al. is the amount of metal participation in the LUMOs

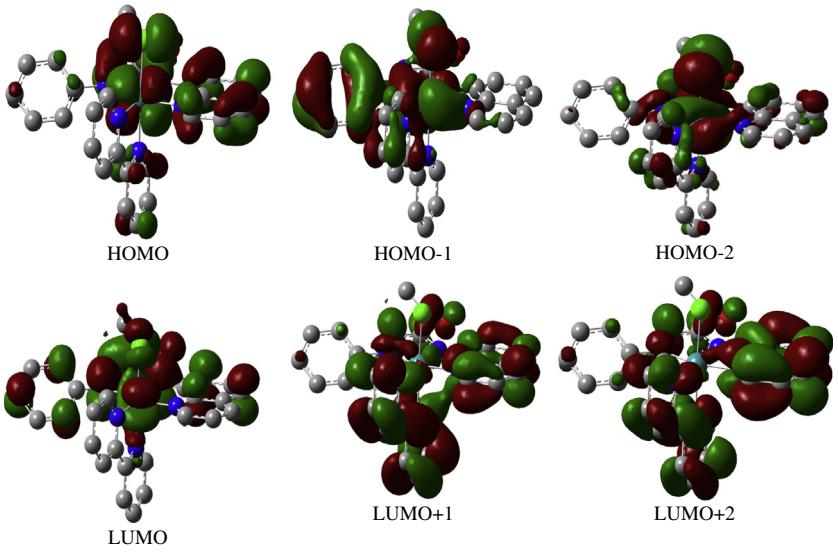

Fig. 4. Isodensity plots of the HOMO and LUMO orbitals of **1**.

Table 4
DFT energies and composition of selected highest occupied and lowest unoccupied molecular orbitals of complex **1** expressed in terms of composing fragments.

MO	eV	Ru	Cl	L—H	bpy
LUMO+10	−0.95	5	10	45	40
LUMO+9	−1.10	5	4	50	41
LUMO+8	−1.15	3	2	75	20
LUMO+7	−1.19	35	35	10	20
LUMO+6	−1.23	2	2	34	60
LUMO+5	−1.29	13	1	6	80
LUMO+4	−1.50	5	1	13	82
LUMO+3	−1.97	3	1	95	1
LUMO+2	−2.44	3	2	55	40
LUMO+1	−2.49	5	3	42	50
LUMO	−3.89	10	10	78	2
HOMO	−6.15	35	11	51	3
HOMO−1	−6.55	51	21	23	5
HOMO−2	−6.67	55	22	22	1
HOMO−3	−6.90	22	15	55	8
HOMO−4	−7.13	10	5	50	35
HOMO−5	−7.17	5	10	45	40
HOMO−6	−7.20	2	10	86	2
HOMO−7	−7.23	3	9	85	2
HOMO−8	−7.26	2	10	85	3
HOMO−9	−7.29	5	25	50	20
HOMO−10	−7.32	7	20	60	13

which can be correlated with π-back donation from the metal d orbitals. They found that the LUMO had over 10% contribution from the metal, but that LUMO+1 and LUMO+2 had little contribution [38]. For the HOMOs, the three highest energy orbitals are Ru in character. These three HOMOs contain a sizeable contribution from azoimine–qinoline and chloride ligands.

On the basis of its intensity and position, the high intensity and energy band at 284 nm (∼293 nm (calculated)) (Table 5) resulted from HOMO−5 to LUMO+2 thus this band is assigned as ligand-to-ligand charge transfer LLCT (π–π^* (phenyl ring) and n–π^* (azomethine (C═N)) transitions. The lowest energy band which is appear as a shoulder at 550 nm (567.7 nm (calculated)) is resulted from HOMO−1/−2 which have a sizable contributions of Ru(dπ) orbitals and chloride to LUMO which has a significant contribution from the π^* orbital of azoimine–quinoline (L—H). The band at 512 nm (∼513 nm (calculated)) is resulted from the (HOMO/−2/−3) orbitals, to LUMO/+3. The band centered at 434 nm (∼408 nm (calculated)) is resulted from HOMO to LUMO+2. Thus all these three bands in the visible region are assigned to metal–ligand-to-ligand charge transfer MLLCT (Ru(dπ), Cl) → L(π^*)) [39–41]. Fig. 5 shows the oxidative spectroelectrochemistry of **1** in dichloromethane. For the oxidation spectrum, there is a complete disappearance of the MLLCT bands at 490 and 530 nm and the appearance of a new band near 650 nm originating from a ligand-to-Ru(III) LMCT transition.

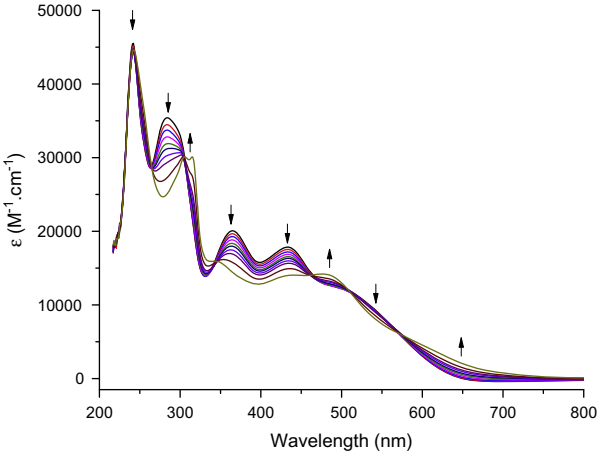

Fig. 5. Spectroelectrochemical experiment showing the absorption spectrum changes upon oxidation of complex **1** in a dichloromethane solution of and 0.1 M TBAHF.

For this family *trans*-[Ru^{II}(L—Y)(bpy)Cl_2] (**1**–**4**), there is an anodic shift for the Ru(III/II) couple and small shift in the energy of the lowest MLCT bands band upon replacing the electron donating group (Y═CH_3) azoimine–qinoline ligands by electron withdrawing groups (Br, NO_2). The small shift can be explained by the small changes in the energy of the orbitals involved in MLLCT (HOMO's and the LUMO azoimine ligand).

Electrochemistry

The electron-transfer behavior of the complexes in dichloromethane solution was examined by cyclic voltammetry and the corresponding results are summarized in Table 3. The Ru(III/II) couples were calculated from average of the $E^{\circ}_{1/2}$ values for the anodic and cathodic waves from cyclic voltammetry. Decamethyl-

Table 5
Computed excitation energies (nm), electronic transition configurations and oscillator strengths (*f*) for the optical transitions in the visible region of complex **1** transition with $f \geqslant 0.02$ are listed).

(nm)	(eV)	*f*.	Major contributions
567.7	2.19	0.04	HOMO−2 → LUMO (43%), HOMO−1 → LUMO (43%)
505.3	2.46	0.25	HOMO−3 → LUMO (84%)
455.7	2.73	0.02	HOMO−4 → LUMO (83%)
434.9	2.86	0.02	HOMO−5 → LUMO (14%), HOMO → LUMO+1 (58%)
418.2	2.97	0.21	HOMO−6 → LUMO (14%), HOMO → LUMO+2 (62%)
408.2	3.04	0.03	HOMO−10 → LUMO (22%), HOMO−8 → LUMO (41%)
386.2	3.22	0.03	HOMO−1 → LUMO+1 (77%)
372.8	3.33	0.02	HOMO−2 → LUMO+1 (53%)
365.6	3.40	0.07	HOMO−11 → LUMO (17%), HOMO−2 → LUMO+2 (45%)
360.5	3.45	0.10	HOMO−2 → LUMO+1 (14%), HOMO−2 → LUMO+2 (32%)
343.7	3.62	0.06	HOMO−12 → LUMO (17%), HOMO → LUMO+4 (40%)
333.8	3.72	0.02	HOMO−12 → LUMO (29%), HOMO−1 → LUMO+4 (30%)
332.5	3.74	0.04	HOMO−12 → LUMO (36%), HOMO−1 → LUMO+4 (45%)
325.3	3.82	0.02	HOMO−3 → LUMO+1 (75%)
323.5	3.84	0.03	HOMO−2 → LUMO+4 (31%), HOMO−2 → LUMO+8 (18%)
319.5	3.89	0.04	HOMO−3 → LUMO+2 (39%), HOMO → LUMO+5 (26%)
317.4	3.91	0.02	HOMO−2 → LUMO+4 (26%), HOMO−2 → LUMO+8 (38%)
295.1	4.21	0.02	HOMO−14 → LUMO (31%), HOMO−13 → LUMO (45%)
293.6	4.23	0.10	HOMO−5 → LUMO+1 (36%)
292.3	4.25	0.02	HOMO−4 → LUMO+2 (64%)
291.3	4.27	0.03	HOMO−5 → LUMO+1 (17%), HOMO−1 → LUMO+5 (25%)

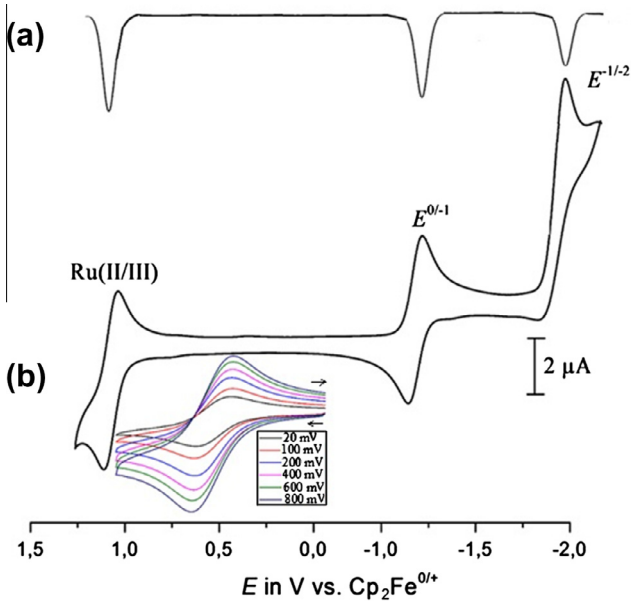

Fig. 6. (a) Differential pulse voltammogram, (b) cyclic voltammogram of complex **1** vs. $Cp_2Fe^{0/+}$ (TBAHF, 0.1M, dichloromethane, 25 °C). Inset shows the Ru(II/III) at different scan rates.

ferrocene was added as an internal standard near the end of the experiment. Ru(III/II) couples was referenced against $Cp_2Fe^{0/+}$ and can be referenced to the NHE by adding 0.62 V [42]. As a representative example, the cyclic voltammogram for complex **1** is shown in Fig. 6b. Complexes **1** exhibited a reversible oxidative response at 0.98 V *vs.* Cp_2Fe/Cp_2Fe^{+}, which has been assigned to Ru(III/II) oxidation. Since the lowest unoccupied molecular orbitals are L—H in character, The two one electron ligand reduction waves between −1.30 and −1.70 V vs. $Cp_2Fe^{0/+}$ (cathodic wave peak maxima) are assigned to the two electron reduction of the azo group. [9–15]. The one-electron oxidation–reduction nature has been established by differential pulse voltammetry (Fig. 6a).

The large anodic shift (~400 mV) for this family compared to the *trans*-[Ru(PhN=NC(COCH$_3$)=NPh)(bpy)Cl$_2$] complexes [8,9] resulted from replacing one of the good donor chloride ligands with moderate π-acceptor pyridine ligand. For this family it is possible to tune the Ru(III/II) couples by 0.34 V upon replacing the CH_3 donor group with NO_2 withdrawing group. The Ru(III/II) couples of the present set of chloro complexes **1**–**4** is more anodic than that of previously reported, [Ru^{II}(trpy)(bpy)Cl] [43–45]. Thus the replacement of two of the pyridine of trpy ligand with strong π-acidic azoimine moiety (N=C—N=N—) [46,47] group lower the energy of the HOMO for ruthenium (II) complexes and shift Ru(III/II) positively compared to similar polypyridine complexes [43–45].

The redox properties of the complex 1 can be explained on the basis of DFT calculations. Oxidation involves electron abstraction from occupied MOs and reduction involves electron addition to unoccupied MOs. Since the HOMO of the complexes has a metal contribution, 35%, oxidation can be regarded as oxidation of the metal center, Ru(II) → Ru(III). Although the ligand (I-H) orbital also contribute significantly in the HOMO, the component does not has electrons to be extracted. On the other hand, the I—H ligand contributes 78% to constitute the LUMO and thus the reduction may be referred as electron accommodation in the π orbital of the azoimine group. The HOMO–LUMO energy gap has also been well correlated with the difference between the first oxidation (refers to the energy of the HOMO) and first reduction (refers to the energy of the LUMO) potentials.

Conclusions

Four ruthenium (II) complexes, [Ru^{II}(L—Y)(bpy)Cl](PF$_6$), where L—Y is a novel NN′N″ tridentate donor ligands which is coordinated to ruthenium via azo (N) imine nitrogen (N′) and quinoline nitrogen (N″) ligands. The complexes have been characterized by spectroscopic, electrochemical and crystallographic of **1**. The ligands H_2L—Y are synthesized in their reduced form and the crystal structures of **1** show that the ligand was oxidized to its azoimine form. The Ru(III/II) couples of these complexes are among the highest reported in ruthenium(II) chemistry and it is possible to tune the couple by 0.34 V upon replacing the CH_3 donor group with NO_2 withdrawing group. The electronic absorption spectra of these complexes show three bands in the Vis region in dichloromethane solution. They are assigned to MLLCT transitions based on TD-DFT calculation.

Acknowledgement

M. Al-Noaimi would like to thank The Hashemite University, Jordan.

Appendix A. Supplementary data

Crystallographic data have been deposited with the Cambridge Crystallographic Data Center; CCDC No. 967681 Copies of this information may be obtained from the director, CCDC, 12 Union Road, Cambridge CB2 1EZ, UK. Tel.: +44 1223 762910; fax: +44 1223 336 033; e-mail: deposit@ccdc.cam.ac.uk or on the web www: http://www.ccdc.cam.ac.uk/deposit. Supplementary data associated with this article can be found, in the online version, at http://dx.doi.org/10.1016/j.saa.2014.01.075.

References

[1] (a) M.A.S. Aquino, Coord. Chem. Rev. 248 (2004) 1025–1045;
(b) S. Rigaut, D. Touchard, P.H. Dixneuf, Coord. Chem. Rev. 248 (2004) 1585–1601;
(c) M.K. Nazeeruddin, S.M. Zakeeruddin, J.-J. Lagref, P. Liska, P. Comte, C. Barolo, G. Viscardi, K. Schenk, M. Graetzel, Coord. Chem. Rev. 248 (2004) 1317–1328;
(d) Md.K. Nazeeruddin, C. Klein, P. Liska, M. Grätzel, Coord. Chem. Rev. 249 (2005) 1460–1467.
[2] (a) K. Hutchison, J.C. Morris, T. Nile, J.L. Walsh, D.W. Thompson, J.D. Petersen, J.R. Schoonover, Inorg. Chem. 38 (1999) 2516–2523;
(b) J. Zadykowicz, P.G. Potvin, Inorg. Chem. 38 (1999) 2434–2441;
(c) R.M. Berger, D.R. McMillin, Inorg. Chem. 27 (1998) 4245–4249;
(d) R.R. Ruminski, S. Underwood, K. Vallely, S.J. Smith, Inorg. Chem. 37 (1998) 6528–6531.
[3] M.K. Nazeeruddin, A. Kay, I. Rodicio, R. Humphry-Baker, E. Mueller, P. Liska, N. Vlachopoulos, M. Graetzel, J. Am. Chem. Soc. 115 (1993) 6382–6390.
[4] H.J. Roth, H. Fenner, In Arzneistoffe 3rd ed., Deutscher Apotheker Verlag: Stuttgart, 2000; pp. 51–114.
[5] (a) T. Wada, K. Tsuge, K. Tanaka, Angew. Chem., Int. Ed. 39 (2000) 1479–1482;
(b) A. El-ghayoury, A. Harriman, A. Khatyr, R. Ziessel, Angew. Chem., Int. Ed. 39 (2000) 185–189;
(c) M. Kurihara, S. Daniele, K. Tasuge, M. Sugimoto, K. Tanaka, Bull. Chem. Soc. Jpn. 71 (1998) 867–875.
[6] B. Mondal, M.G. Walawalkar, G.K. Lahiri, J. Chem. Soc., Dalton Trans. (2000) 4209–4217.
[7] C.R. Harris, A. Thorarensen, Curr. Med. Chem. 11 (2004) 2213–2243.
[8] M. Al-Noaimi, H. Saadeh, S. Haddad, M. El-Barghouthi, M. El-khateeb, R.J. Crutchley, Polyhedron 26 (2007) 3675–3685.
[9] M. Al-Noaimi, M. El-khateeb, S. Haddad, M. Sunjuk, R. Crutchley, Polyhedron 27 (2008) 3239–3246.
[10] M. Al-Noaimi, R. Abdel-Jalil, S. Haddad, R. Al-Far, M. Sunjuk, R.J. Crutchley, Inorg. Chim. Acta 359 (2006) 2395–2399.
[11] M. Al-Noaimi, R.J. Crutchley, M. AlDamen, A. Rawashdeh, M.A. Khanfar, K. Seppelt, Polyhedron 30 (2011) 2075–2082.
[12] M. Al-Noaimi, M.A. AlDamen, Inorg. Chim. Acta 387 (2012) 45–51.
[13] M. Al-Noaimi, M. El-khateeb, I. Warad, S.F. Haddad, Inorg. Chim. Acta 400 (2013) 20–25.
[14] M. Al-Noaimi, M. Sunjuk, M. El-khateeb, S.F. Haddad, A. Haniyeh, M. AlDamen, Polyhedron 42 (2012) 66–73.

[15] M. Al-Noaimi, M. El-khateeb, S. Haddad, H. Saadeh, Tran. Met. Chem. 35 (2010) 877–883.
[16] M. Krejcik, M. Danek, F. Hartl, J. Electroanal. Chem. 317 (1991) 179–187.
[17] C. Nataro, A.N. Campbell, M.A. Ferguson, C.D. Incarvito, A.L. Rheingold, J. Organomet. Chem. 673 (2003) 47–55.
[18] T. Gennett, D.F. Milner, M.J. Weaver, J. Phys. Chem. 89 (1985) 2787–2794.
[19] C. Lee, W. Yang, R.G. Parr, Phys. Rev. B 37 (1988) 785–789.
[20] M.J. Frisch et al., Gaussian 03, Revision D.01, Gaussian Inc, Wallingford CT, 2004GaussView3.0, Gaussian: Pittsburgh, PA.
[21] P.J. Hay, W.R. Wadt, J. Chem. Phys. 82 (1985) 270–283.
[22] R. Bauernschmitt, R. Ahlrichs, Chem. Phys. Lett. 256 (1996) 454–464.
[23] M.K. Casida, C. Jamorski, K.C. Casida, D.R. Salahub, J. Chem. Phys. 108 (1998) 4439–4449.
[24] R.E. Stratmann, G.E. Scuseria, M.J. Frisch, J. Chem. Phys. 109 (1998) 8218–8224.
[25] M. Cossi, N. Rega, G. Scalmani, V. Barone, Comput. Chem. 24 (2003) 669–681.
[26] N.M. O'Boyle, A.L. Tenderholt, K.M. Langner, J. Comput. Chem. 29 (2008) 839–845.
[27] CrysAlisPro, Agilent Technologies, Version 1.171.35.11 (Release 16–05–2011 CrysAlis171.NET) (Compiled May 16 2011,17:55:39).
[28] SHELXTL (XCIF, XL, XP, XPREP, XS), version 6.10, Bruker AXS Inc.: Madison, WI, 2002.
[29] (a) A. Spek, A. Gerli, J. Reedjik, Acta Crystallogr., Sect. C 50 (1994) 394–397; (b) N.C. Pramanik, K. Pramanik, P. Ghosh, S. Bhattacharya, Polyhedron 17 (1998) 1525–1534.
[30] B.K. Santra, G.A. Thakur, P. Ghosh, A. Pramanik, G.K. Lahiri, Inorg. Chem. 35 (1996) 3050.
[31] C.J. Cathey, E.C. Constable, M.J. Hannon, D.A. Tocher, M.D. Ward, J. Chem. Soc., Chem. Commun. (1990) 621–623.
[32] J. Dinda, K. Bag, C. Sinha, G. Mostafa, T.-H. Lu, Polyhedron 22 (2003) 1367–1376.
[33] M. Al-Noaimi, B.F. Ali, A. Rawashdeh, Z. Judeh, Polyhedron 29 (2010) 3214–3219.
[34] M. Al-Noaimi, M. El-khateeb, H. Görls, Acta Crystallogr., Sect. E 63 (11) (2007) m2713.
[35] (a) R.M. Silverstein, G.C. Bassler, T.C. Morrill, Spectrometric Identification of Organic Compounds, Wiley, New York, 1981; (b) B.H. Chen, H.H. Yao, W.T. Huang, P. Chattopadhyay, J.M. Lo, T.H. Lu, Solid-State Sci. 1 (1999) 119–131.
[36] D.A. Bardwell, A.M.W. Cargill Thompson, J.C. Jeffery, J.A. McCleverty, M.D. Ward, J. Chem. Soc., Dalton Trans. (1996) 873–878.
[37] (a) E.M. Kober, T.J. Meyer, Inorg. Chem. 21 (1982) 3967–3977; (b) A. Ceulemans, L.G. Vanquickenberne, J. Am. Chem. Soc. 103 (1981) 2238–2241.
[38] S.I. Gorelsky, A.B. Lever, M. Ebadi, Coord. Chem. Rev. 230 (2002) 97–105.
[39] D.J. Stufkens, A. Vlček, J. Coord. Chem. Rev. 177 (1998) 127–179.
[40] H.A. Nieuwenhuis, D.J. Stufkens, A. Oskam, Inorg. Chem. 33 (1994) 3212–3217.
[41] B.D. Rossenaar, D.J. Stufkens, A. Vlček, J. Inorg. Chem. 35 (1996) 2902–2909.
[42] S. Lu, V.V. Strelets, M.F. Ryan, W.J. Pietro, A.B.P. Lever, Inorg. Chem. 35 (1996) 1013–1023.
[43] K.J. Takeuchi, M.S. Thompson, D.W. Pipes, T.J. Meyer, Inorg. Chem. 23 (1984) 1845–1851.
[44] M. Al-Noaimi, G. Yap, R.J. Crutchley, Inorg. Chem. 43 (5) (2004) 1770–1778.
[45] A.B.P. Lever, Inorg. Chem. 29 (1990) 1271–1285.
[46] S. Pal, D. Das, C. Sinha, C.H.L. Kennard, Inorg. Chim. Acta 313 (2001) 21–29.
[47] P. Byabartta, S. Pal, T.K. Misra, C. Sinha, F.-L. Liao, K. Panneerselvam, T.-H. Lu, J. Coord. Chem. 55 (2002) 479–495.